pubs.acs.org/acschemicalbiology

Articles

Chemoproteomic Profiling of Protein Substrates of a Major Lysine Acetyltransferase in the Native Cellular Context

Jiabao Song, Liza Ngo, Kaylyn Bell, and Y. George Zheng*

Cite This: https://doi.org/10.1021/acschembio.1c00935

Read Online

ACCESS | Metrics & More | Article Recommendations | Supporting Information

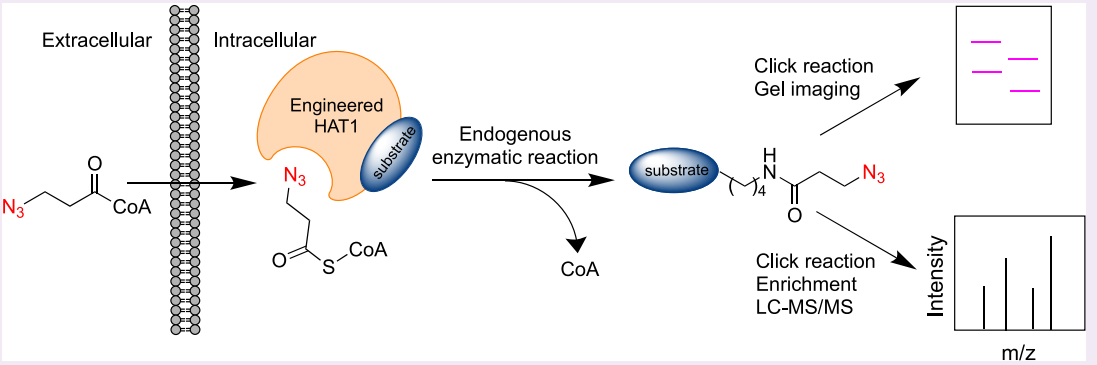

ABSTRACT: The family of lysine acetyltransferases (KATs) regulates epigenetics and signaling pathways in eukaryotic cells. So far, knowledge of different KAT members contributing to the cellular acetylome is limited, which limits our understanding of biological functions of KATs in physiology and disease. Here, we found that a clickable acyl-CoA reporter, 3-azidopropanoyl CoA (3AZ-CoA), presented remarkable cell permeability and effectively acylated proteins in cells. We rationally engineered the major KAT member, histone acetyltransferase 1 (HAT1), to generate its mutant forms that displayed excellent bio-orthogonal activity for 3AZ-CoA in substrate labeling. We were able to apply the bio-orthogonal enzyme−cofactor pair combined with SILAC proteomics to achieve HAT1 substrate targeting, enrichment, and proteomic profiling in living cells. A total of 123 protein substrates of HAT1 were disclosed, underlining the multifactorial functions of this important enzyme than hitherto known. This study demonstrates the first example of utilizing bio-orthogonal reporters as a chemoproteomic strategy for substrate mapping of individual KAT isoforms in the native biological contexts.

INTRODUCTION

Among the diverse post-translational modifications (PTMs), lysine acetylation is versatile and has been linked to various aspects of cellular processes from chromatin remodeling, DNA repair, and signal transduction, to cellular metabolism.[1] High-resolution mass spectrometry-based proteomic analysis has disclosed thousands of acetylation targets and acetylation sites in all subcellular organelles, which include the nucleus, cytosol, mitochondrion, and endoplasmic reticulum, highlighting the widespread engagement of lysine acetylation in regulating cell physiology.[2,3] Site-selective lysine acetylation in protein substrates is dominantly catalyzed by protein lysine acetyltransferases (KATs), which transfer the acetyl group from acetyl-coenzyme A (acetyl-CoA, Ac-CoA) to the epsilon-amino group of lysine residues.[4] Lysine acetylation marks can be recognized by "reader" proteins, connecting this modification to downstream signaling networks.[5] A dozen of KAT members have been identified and classified into different major families including the GNAT family, the MYST family, and the p300/CBP family. HAT1, which belongs to the GNAT superfamily, was one of the first discovered KATs in the mid-1990s.[6] Renewed attention to HAT1 was witnessed in recent years owing to its functional association with diverse oncologic processes.[7]

Biochemical and cellular studies show that HAT1 acetylates newly synthesized histone H4 at K5 and K12 sites,[8] as well as histone H2A at the K5 site in the cytoplasm.[9] Taken into account the thousand-sized acetylome and the extensive correlation of HAT1 with disease processes, it is proposed that the substrate profile of HAT1 could be much broader than merely nuclear histones, a scope beyond the chromatin regulation.[10] To fully illuminate the significance of lysine acetylation and HAT1 functions in regulating epigenetics, signaling cascades, and disease pathways, it is critical to identify

Received: November 26, 2021
Accepted: March 30, 2022

Table 1. Structures of the Azide- or Alkyne-Functionalized Fatty Acids and Acyl-CoAs That were Used for the Cell Permeability Detection

Structures of acetate analogs	Names of the acetate analogs	Structures of corresponding acyl-CoA analogs	Abbreviated names of the acyl-CoA analogs
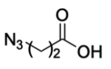	3-azidopropanoic acid (3AZ-acid)	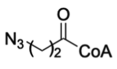	3AZ-CoA
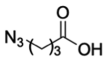	4-azidobutyric acid (4AZ-acid)	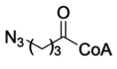	4AZ-CoA
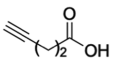	4-pentynoic acid (4PY-acid)	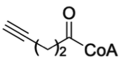	4PY-CoA
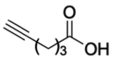	5-hexynoic acid (5HY-acid)	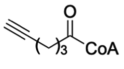	5HY-CoA
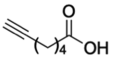	6-heptynoic acid (6HY-acid)	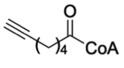	6HY-CoA

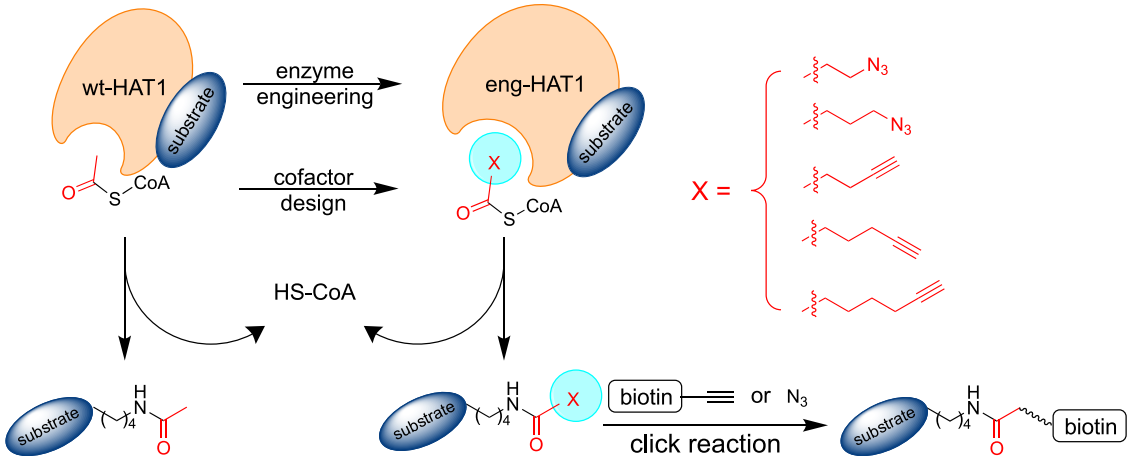

Figure 1. Schematic description of eng-HAT1 combined with acyl-CoA analogues to label HAT1 substrates. The Ac-CoA binding pocket of wild-type HAT1 was rationally expanded by mutation of selected amino acid residues to accommodate bulkier acyl-CoA analogues. The transferrable azido or alkyne moiety can further be detected via a click reaction-induced biotin probe.

the molecular targets of HAT1 on the proteomic scale in the cellular context.

Earlier approaches to profiling individual KAT substrates typically rely on immunoprecipitation of acetylated proteins or peptides from cells pretreated with genetic knockdown or selective KAT inhibitors.[11−13] For instance, Garcia et al. recently identified 65 HAT1-dependent acetylation proteins with 84 sites by comparing immortalized $HAT1^{+/+}$ and $HAT1^{-/-}$ mouse embryonic fibroblast cell lines (MEFs).[13] These methods are effective but have some inherent drawbacks such as the functional redundancy of many HATs. One might expect that when a particular HAT member is knocked out but another redundant HAT acetylates its substrates, those substrates will be invisible in knockout experiments. Importantly, the PTM antibody-based immunoprecipitation is often compromised by issues such as limited sequence diversity, promiscuous cross-reactivity, and batch- and source-caused disparities, which may lead to incomplete enrichment and/or high background signals.[14] Moreover, many KATs possess promiscuous acyltransferase activities, not merely acetylation.[15,16] Besides lysine acetylation, HAT1 was recently found to transfer succinyl, propionyl, isobutyryl, and methacrylyl groups to its substrates.[17−19] It would be projected that incomplete substrates are detected when solely using an acetyllysine antibody to enrich protein substrates of KATs. As such, it is of great demand to develop new and alternative approaches for the identification and profiling of KAT substrates.

In recent years, functionalized acyl-CoA reporters, particularly those bearing small-sized and chemoselective warhead groups, have been developed and applied for the identification of lysine acylated substrates.[4,20] Yu et al. used chloroacetyl-CoA as an orthogonal probe to label HAT1 substrates in vitro, but low efficiency and specificity as well as poor cell

https://doi.org/10.1021/acschembio.1c00935
ACS Chem. Biol. XXXX, XXX, XXX−XXX

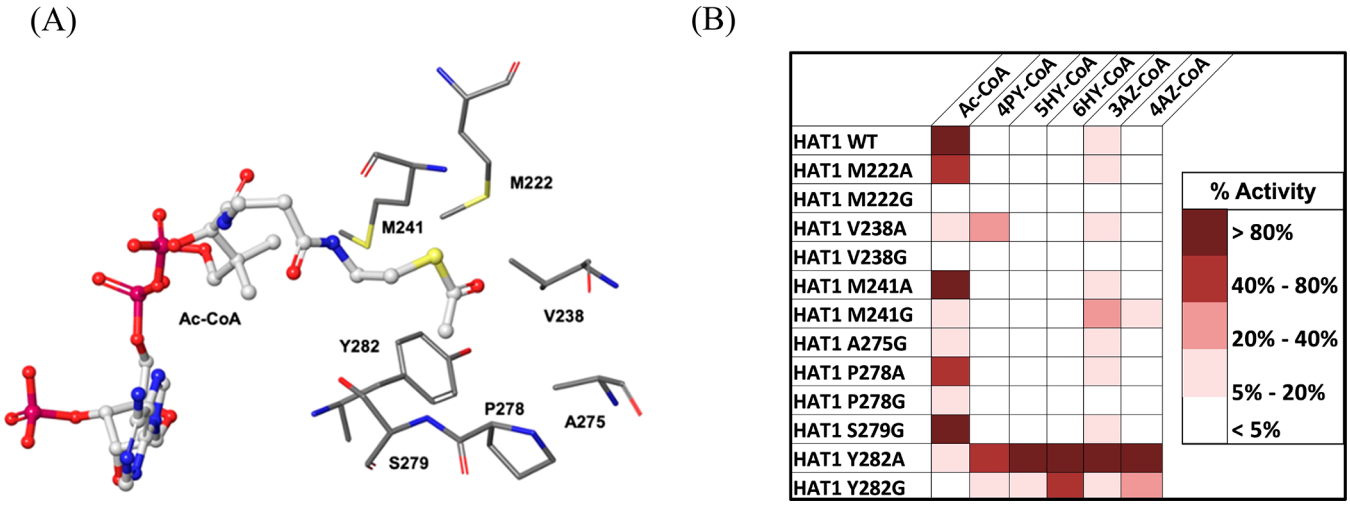

Figure 2. Investigation of wt or eng-HAT1 activities toward different acyl-CoA analogues. (A) Targeted hydrophobic bulky residues surrounding the Ac-CoA active site of HAT1-catalyzed acetylation for HAT1 engineering. (PDB file: 2P0W). (B) Enzymatic activity of HAT1 and its various mutants toward Ac-CoA and its analogues.

permeability limit its further application in the global elucidation of HAT1 substrates in a cellular context.[21] Lyu et al.[22] recently used fluoroacetyl-CoA in combination with reactive thiol agents to label KAT substrates. We and others have made and applied acyl-CoA reporters for KAT substrates' discovery that bear azido or alkynyl functional groups, such as 3-azidopropanoyl CoA (3AZ-CoA), 4-azidobutanoyl CoA (4AZ-CoA), 4-pentynoyl CoA (4PY-CoA), 5-hexynoyl CoA (5HY-CoA), and 6-heptynoyl CoA (6HY-CoA) (Table 1). Several of these acyl-CoA reporters were shown to be excellent Ac-CoA surrogates to label protein substrates of the KATs either in recombinant proteins or in the complex proteomes of whole-cell lysates.[23−25] However, the lack of native cellular contexts poses a restriction on the accuracy and physiological relevance of substrate discovery. Taking advantage of the bump-and-hole approach,[26,27] herein we attempted to create engineered HAT1 (eng-HAT1) forms that are capable to use bio-orthogonal acyl-CoA reporters to label HAT1 substrates with an azido or alkynyl-containing acyl group, and then, the labeled substrates are conjugated with biotin tag for further optical detection or proteomic analysis (Figure 1). In the process, we investigated the cell permeability of a panel of acyl-CoA bio-orthogonal reporters to identify membrane-penetrating ones for intracellular use. Combined, we applied the eng-HAT1 with its paired cell-permeable bio-orthogonal reporter to label and detect HAT1 substrates in the native cellular environment. We successfully identified hundreds of HAT1 substrates, most of which are previously unknown.

RESULTS AND DISCUSSION

Generating Eng-HAT1 Forms Conferring New Activities for Bio-orthogonal Acyl-CoA Reporters. Clickable acyl-CoA compounds containing azido or alkynyl groups (e.g., 3AZ-CoA, 4AZ-CoA, 4PY-CoA, 5HY-CoA, and 6HY-CoA) have been recently designed as cofactors to label peptide and protein substrates for different KATs.[23−25] To identify the potential protein substrates of HAT1 with bio-orthogonal reporters, we wondered whether wild-type (wt) HAT1 can utilize these un-natural acyl-CoAs for substrate labeling. After analyzing the crystal structure of the HAT1-Ac-CoA complex (Figure 2A, PDB: 2P0W),[28] we surmise that the active pocket is too narrow to accommodate the bulky acyl group of acyl-CoA. Therefore, we adopted a bump-and-hole approach to mutate the residues bordering the Ac-CoA binding site of HAT1 to expand the space surrounding the acetyl group (Figure 1), with the goal of obtaining some mutant forms that can accommodate the synthetic acyl-CoA reporters. We identified seven bulky amino acid residues in the Ac-CoA binding pocket of HAT1, i.e., M222, V238, M241, A275, P278, S279, and Y282. Each of these residues was mutated to a less sterically hindered amino acid, i.e., alanine or glycine (Figure 2A). It is our hope that, as a result of the mutation, the expanded binding pocket will be able to tolerate the larger size of acyl-CoA analogues, leading to deposition of azido- or alkynyl-acyl moiety to the substrates of HAT1. Therefore, by using the pET28a-HAT1 (20−341) plasmid (Addgene, plasmid# 25239) as a template, we mutated each of the selected residues to alanine or glycine using the QuikChange site-directed mutagenesis protocol (Supporting Table S1). By protein expression in *Escherichia coli* BL21(DE3) cells and followed by Ni-NTA affinity purification, we successfully obtained the recombinant wt-HAT1 and different eng-HAT1 proteins (SDS-PAGE of the expressed proteins were shown in Supporting Figure S1).

Screening Acyltransferase Activities of wt- and Eng-HAT1 Toward Acyl-CoA Reporters. The acyl transfer activities of wt-HAT1 and the HAT1 mutants were measured by quantifying the side product CoA using the fluorogenic probe 7-diethylamino-3-(4'-maleimidylphenyl)-4- methylcoumarin (CPM).[29,30] In a typical procedure, reactions containing 0.04 μM of the wt or eng-HAT1 enzyme were incubated with 40 μM of the N-terminal 20 amino acid H4 peptide, H4 (1-20), and individual acyl-CoA analogues (20 μM). The reactions were quenched with CPM (60 μM) in DMSO and then incubated in total darkness for 20 min in room temperature. Fluorescence was measured at an excitation and emission wavelength of 392 and 482 nm, respectively. The data were summarized in the heat map format (Figure 2B and Supporting Figure S2).

As expected, wt-HAT1 showed desired acetyl transfer activity toward Ac-CoA but almost no detectable activities for other acyl-CoA cofactors. This testifies to our premise that

https://doi.org/10.1021/acschembio.1c00935
ACS Chem. Biol. XXXX, XXX, XXX−XXX

the active site of HAT1 is too narrow to accommodate the bulky size acyl groups. In contrast, different HAT1 mutants exhibited varied activities toward azide/alkyne acyl-CoAs. When P278 was mutated to Gly, there was only 10% activity for Ac-CoA and none for the other cofactors. However, when replaced with an Ala, the activity for Ac-CoA increased to 40% and there was 10% activity for 3AZ-CoA. This suggests that a residue with a hydrophobic side chain is needed at this position to aid in the stabilization of the acyl group binding.[28] The same phenomenon observed was seen with HAT1-Y282: the methyl side chain of Ala in HAT1-Y282A was observed to increase the acyltransferase activity greatly in comparison to HAT1-Y282G. HAT1-Y282G had 1% activity with Ac-CoA, less than 17% activity with 4PY-CoA, 5HY-CoA, and 3AZ-CoA, about 20% activity with 4AZ-CoA, and the highest activity at 50% with 6HY-CoA. In comparison, HAT1-Y282A had about 6% activity with Ac-CoA, 61% activity with 4PY-CoA, and greater than 80% activity with most of the acyl-CoA reporters such as 5HY-CoA, 6HY-CoA, 3AZ-CoA, and 4AZ-CoA. Remarkably, HAT1-Y282A was almost inert to Ac-CoA compared to its high activity toward the synthetic acyl-CoA cofactors. Given this orthogonal feature, we chose the HAT1-Y282A mutant for further substrate detection for HAT1.

To confirm HAT1-Y282A's activities toward the acyl-CoA reporters in histone H4 acylation, the mixtures of the enzymatic reaction of HAT1-Y282A, acyl-CoA analogues, and H4 peptide (H4 (1-20)) were analyzed by MALDI-MS. As shown in Supporting Figure S3, the H4 (1-20) was clearly acylated by the acyl-CoA analogues, which is consistent with the above CPM assay results. Next, we quantitatively measured the steady-state kinetic rates of HAT1-Y282A in H4 labeling with the acyl-CoA analogues at a series of concentrations by using the CPM assay. The kinetic constants k_{cat} and K_m were determined by fitting the acyl-CoA concentration-catalytic rate to the Michaelis–Menten equation. k_{cat}/K_m was calculated to evaluate the catalytic efficiency for each acyl-CoA analogue (Table 2 and Supporting Figure S4). In particular, HAT1-Y282A exhibited extremely high activities toward 6HY-CoA and 3AZ-CoA with k_{cat}/K_m values of 1.40 and 1.08 $min^{-1}\mu M^{-1}$, respectively. Moderate activities were shown against 5HY-CoA, 4AZ-CoA, and 4PY-CoA (k_{cat}/K_m: 0.84, 0.76, and 0.30 $min^{-1}\mu M^{-1}$), yet HAT1-Y282A was almost inert toward the natural cofactor Ac-CoA (k_{cat}/K_m: 0.03 $min^{-1}\mu M^{-1}$). Collectively, the results support that the engineered enzyme HAT1-Y282A had obtained excellent activities and orthogonal preference toward the synthetic azide/alkyne acyl-CoA reporters for HAT1 substrate labeling.

Table 2. Kinetic Analysis of HAT1-Y282A Activity Against acyl-CoA Analogues[a]

cofactor	k_{cat} (min^{-1})	K_m (μM)	k_{cat}/K_m ($min^{-1}*\mu M^{-1}$)
6HY-C0A	33.2 ± 2.3	23.7 ± 5.2	1.40
3AZ-CoA	11.1 ± 0.3	10.3 ± 1.2	1.08
5HY-CoA	9.8 ± 0.8	11.7 ± 2.6	0.84
4AZ-CoA	13.15 ± 0.6	17.4 ± 2.6	0.76
4PY-CoA	25.4 ± 0.8	85.9 ± 5.9	0.30
Ac-CoA	NA	>200	0.03[b]

[a]Kinetics in the presence of varying concentrations of CoA analogues was obtained by fitting data points to the Michaelis–Menten equation. To determine the kinetics of HAT1-Y282A against various acyl-CoA analogues, reactions containing 40 nM HAT1-Y282A, 200 μM H4 (1-20) peptide, and 0–200 μM various acyl-CoA analogues were incubated for 15 min at 30 °C. [b]This k_{cat}/K_m value was determined by its slope.

In-Gel Imaging of Labeled Substrates by HAT1-Y282A and Acyl-CoA Reporters. We sought to further validate the activities of HAT1-Y282A toward the azide/alkyne acyl-CoA cofactors by examining the labeling efficiency on histone H4 using an imaging mode. Recombinant histone H4 protein was incubated with 6HY-CoA, 3AZ-CoA, and 4AZ-CoA in the presence of HAT1-Y282A. The mixture was then reacted with azido- or alkynyl-biotin by copper-catalyzed azide–alkyne cycloaddition (CuAAC) reaction followed by SDS-PAGE gel separation. The biotinylated H4 was visualized via streptavidin-HRP chemiluminescent imaging. The biotinylated bands of H4 only showed up with the mixture containing HAT1-Y282A and acyl-CoA analogues, but barely any labeling was seen from the groups where HAT1-Y282A was absent (Figure 3). To determine if HAT1-Y282A acylates histone H4 in a site-dependent manner, we synthesized three peptides, e.g., H4 (1-20), H4 (1-22), and H4 (15-38) for labeling detection. As shown in Supporting Figure S5, strong fluorescence was clearly seen within H4 (1-20) and H4 (1-22), but no detectable fluorescence was found for peptide H4 (15-38). This result was consistent with the fact that HAT1 acetylates H4 at K5 and K12 sites.[6,8] These in-gel imaging data further support the bio-orthogonal activities of HAT1-Y282A to the acyl-CoA reporters and demonstrate the feasibility and robustness to use HAT1-Y282A paired with acyl-CoA reporters to identify and image HAT1 cellular substrates.

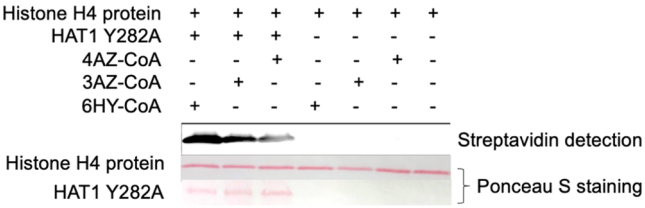

Figure 3. Streptavidin detection of HAT1-Y282A substrate histone H4. Recombinant histone H4 was incubated with HAT1-Y282A paired with 6HY-CoA, 3AZ-CoA, or 4AZ-CoA, followed by conjugation with alkyne-biotin with CuAAC reaction, and imaged by streptavidin-HRP.

Identification of 3AZ-CoA as a Cell-Permeable Bio-orthogonal Reporter. Previously, some engineered KATs combined with bio-orthogonal acyl-CoA reporters have been reported to identify KATs substrates from cell lysates.[24] Lack of native cellular environment, however, potentially compromises substrate labeling efficiency and accuracy. As such, having validated the activity of the HAT1-Y282A mutant toward acyl-CoA reporters on the known HAT1 substrate H4, we attempted to investigate potential cell-permeable acyl-CoA reporters that can be applied to profile HAT1 substrates in living cells. Short-chain fatty acids are known to enter the mammalian cells and metabolically be transformed to their corresponding acyl-CoA, which are utilized by endogenous KATs to install the functional groups to their protein substrates.[2,23] However, the membrane-penetrating efficiency of short-chain fatty acids is typically quite low.[2] Interestingly, a recent study shows that extracellular CoA can adjust intracellular CoA levels.[31] We thus conducted a comparative study of a panel of azide- or alkyne-containing short-chain fatty

https://doi.org/10.1021/acschembio.1c00935
ACS Chem. Biol. XXXX, XXX, XXX–XXX

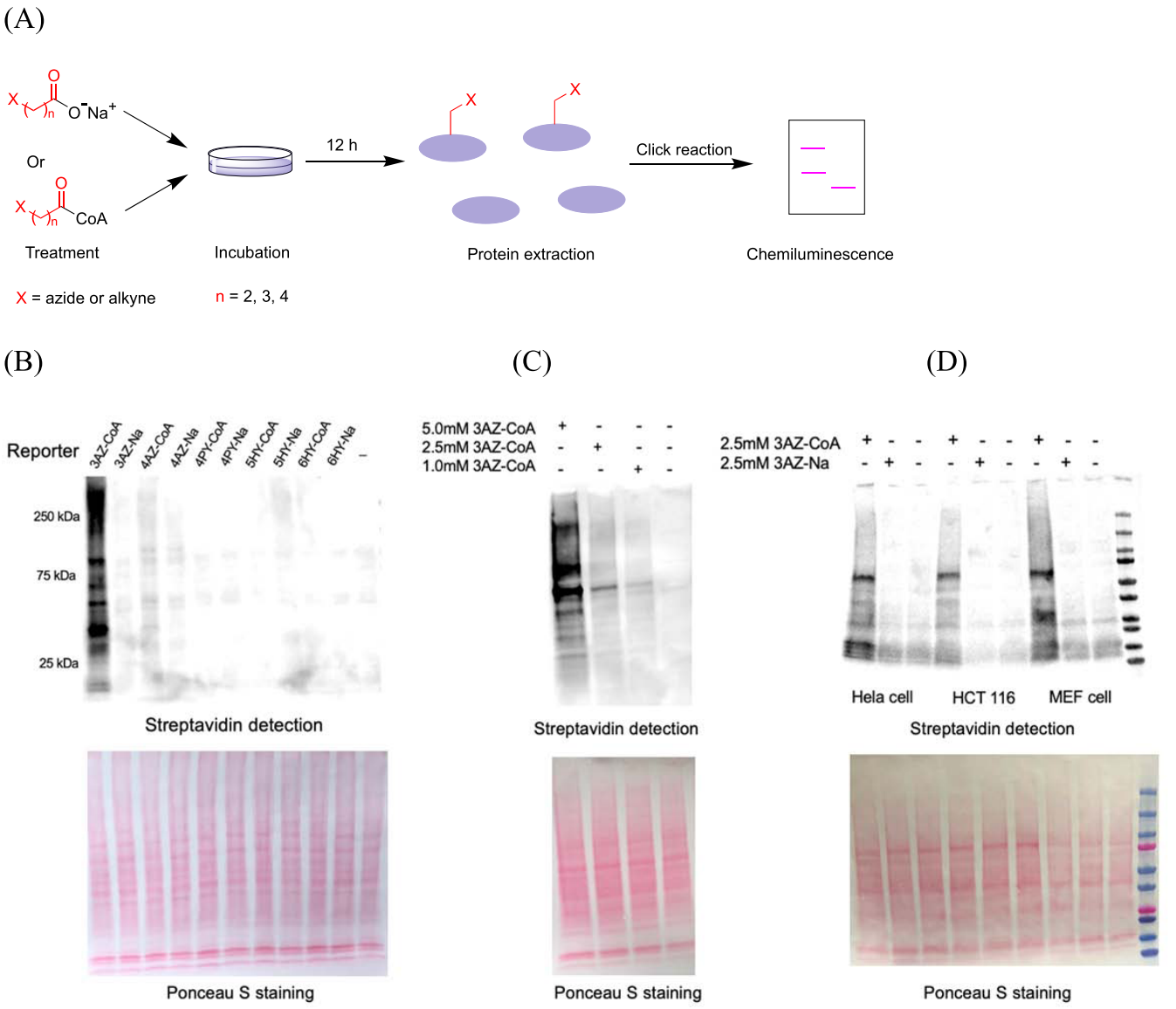

Figure 4. Evaluation of potential cell-permeable bio-orthogonal reports for in vitro protein labeling. (A) Scheme for cellular analysis of cell permeability of bio-orthogonal reporters. (B) Chemoproteomic cellular protein labeling by acetate analogues and acyl-CoA analogues in HEK293T cells. Cells were incubated with different analogues (2.5 mM, 12 h), followed by CuAAC reaction. (C) Dose-dependent labeling of HEK293T cells by 3AZ-CoA. Cells were incubated with 3AZ-CoA as indicated concentration for 12 h. (D) Various cell lines were labeled with 3AZ-CoA and 3AZ-Na. Different cells were incubated with 2.5 mM 3AZ-CoA or 3AZ-Na for 12 h.

acids and acyl-CoA reporters to evaluate their cell membrane permeability and cellular protein labeling sensitivity (Table 1). Individual compounds were added to the culture medium of the human embryonic kidney (HEK) 293T cells at 2.5 mM and incubated for 12 h. Cells were washed with PBS, harvested and lysed in M-PER buffer with sonication, and subjected to CuAAC reaction to conjugate with alkyne-biotin or azide-biotin. The proteins were resolved by SDS-PAGE, and labeled proteins were visualized with streptavidin-HRP (Figure 4A). To our surprise, among all of the tested compounds, 3AZ-CoA turned out to show the most intense protein labeling, and 4AZ-CoA had moderate labeling, while other acyl-CoA analogues and the SCFA compounds exhibited very low levels of protein labeling (Figure 4B). The poor protein labeling by SCFA coincides with the previous study.[2] This result suggests the potential for 3AZ-CoA to serve as a cell-permeable bio-orthogonal reporter for KAT substrate labeling. To validate the cell permeability of 3AZ-CoA, we extracted acyl-CoAs from the cell lysate and used LC-MS/MS to detect the intracellular 3AZ-CoA. Indeed, the signal of intracellular 3AZ-CoA was clearly detected in the cell sample treated with 3AZ-CoA (Supporting Figure S6). By contrast, we cannot detect any MS/MS signal of 3AZ-CoA formation from the 3AZ-Na treatment. This result confirms the excellent cell permeability of 3AZ-CoA to the HEK293T cell.

To gain further insight into the cellular protein labeling by 3AZ-CoA, a dose-dependent treatment of the HEK293T cell with 3AZ-CoA was conducted. We clearly observed that protein labeling grew stronger when 3AZ-CoA concertation increased from 0, 1, 2.5, to 5 mM (Figure 4C). This result again supports the excellent cell permeability of 3AZ-CoA as a bio-orthogonal reporter for KATs. We also evaluated the cytotoxicity of 3AZ-CoA, and only a minor level of cell toxicity was seen at a concentration of 2.5 mM (Supporting Figure S7).

https://doi.org/10.1021/acschembio.1c00935
ACS Chem. Biol. XXXX, XXX, XXX−XXX

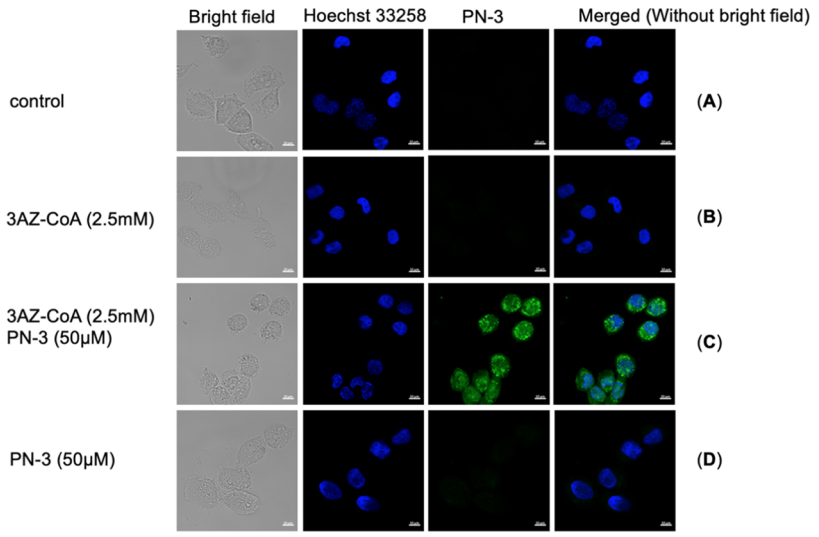

Figure 5. Confocal fluorescence images of HeLa cells with the indicated concentration of 3AZ-CoA and PN-3. (A) Control group. (B) Cells were only treated with 2.5 mM 3AZ-CoA for 12 h without PN-3. (C) Cells were pretreated with 2.5 mM 3AZ-CoA for 12 h and subsequently treated with 50 μM PN-3 for 2 h. (D) Cells were only treated with 50 μM PN-3 for 2 h. Fluorescence images were obtained with a Zeiss LSM 710 Confocal Microscope. Scale bar: 10 μm.

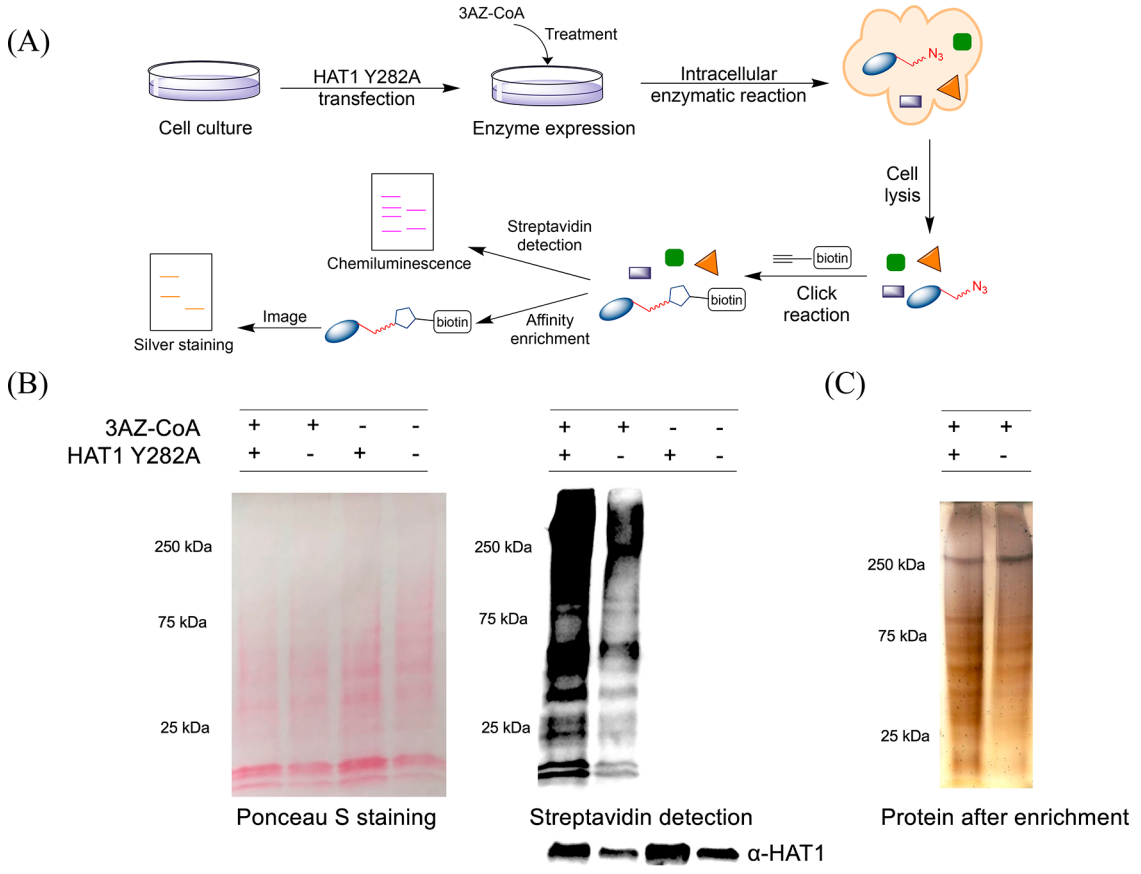

Figure 6. Label HAT1 substrates under the native cellular environment and subsequent protein enrichment. (A) Schematic description of labeling intracellular HAT1 substrates by enzyme overexpression, bio-orthogonal reporter treatment, click reaction, and affinity enrichment. (B) Streptavidin detection of HAT1 cellular substrates in HEK293T cells with HAT1-Y282A overexpression and cell-permeable bio-orthogonal reporter 3AZ-CoA treatment followed by reaction with alkyne-biotin. (C) Enrichment of biotinylated protein by streptavidin beads followed by $Na_2S_2O_4$ cleavage. The protein eluents were resolved on SDS-PAGE and imaged by silver staining.

Next, we sought to test the generality of 3AZ-CoA as a cell-permeable reporter in different kinds of cell lines. HeLa cells, HCT 116 cells, and MEF cells were used to test the cellular protein labeling (Figure 4D). Interestingly, in all of the tested cell lines, 2.5 mM 3AZ-CoA treatment induced much stronger protein labeling compared to either the negative controls (no treatment) or the 2.5 mM 3AZ-Na treatment. Clearly, the cell permeability of 3AZ-CoA is outstanding and versatile. Of note

https://doi.org/10.1021/acschembio.1c00935
ACS Chem. Biol. XXXX, XXX, XXX−XXX

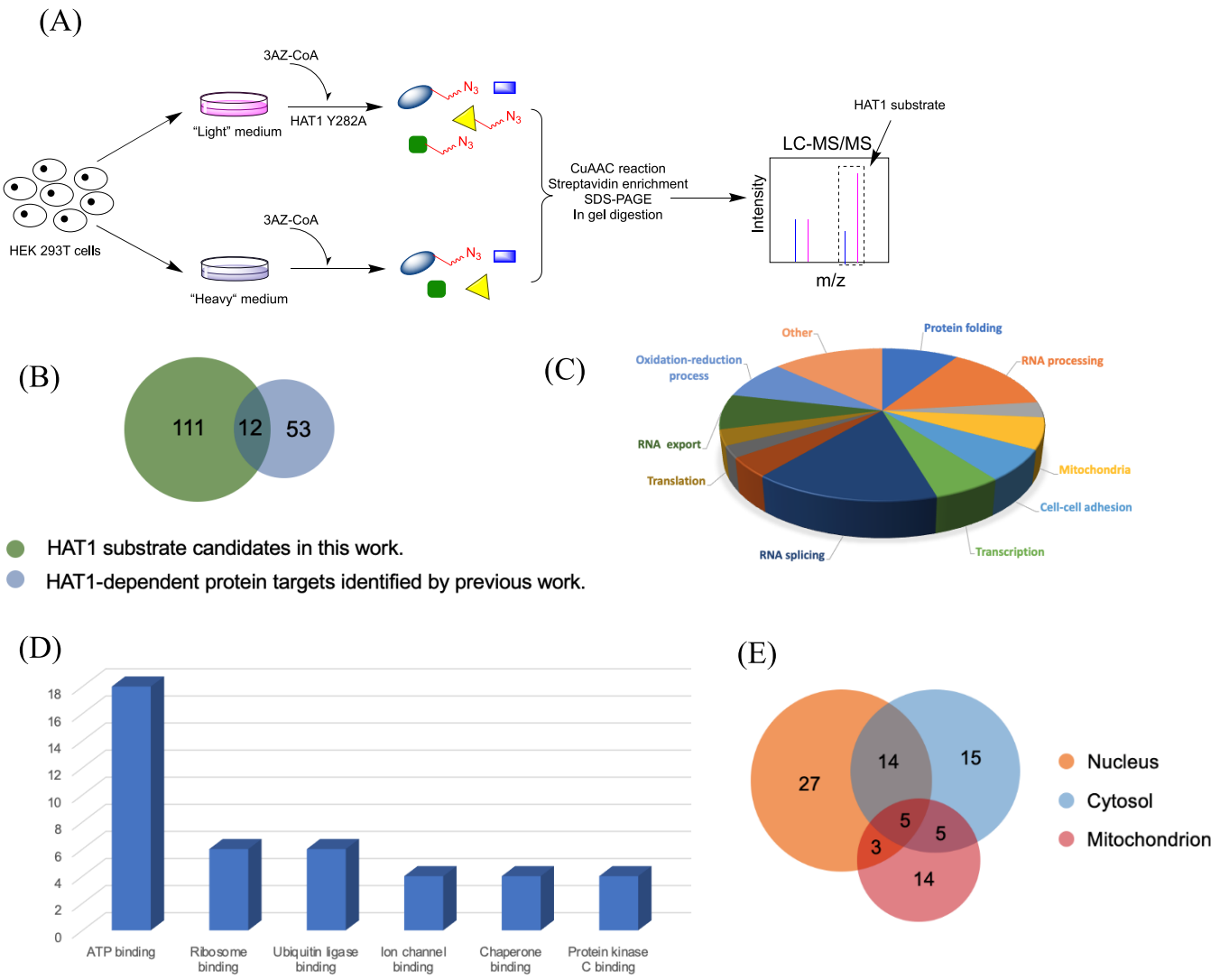

Figure 7. Identification and functional annotation of HAT1 substrates. (A) Schematic illustration of the SILAC proteomics study to identify HAT1 substrates. (B) Identified HAT1 substrates were compared with previously identified HAT1-dependent protein targets. (C) Representative biological processes' annotation for HAT1 substrates. (D) HAT1 substrates show different binding activities. (E) Venn diagram shows cellular compartment distribution of HAT1 substrates.

is that there appeared to be different patterns of protein labeling for each cell line, which suggests distinctive cellular acylations in different cells. Together, our data demonstrate the capability of 3AZ-CoA to be a cell-permeable reporter for KAT substrate labeling.

Having successfully demonstrated 3AZ-CoA as a cell-permeable acylation reporter, we then proceeded to test cellular imaging of protein labeling using the HeLa cell model. Herein, an azide-sensitive turn-on fluorescence probe was chosen to induce live-cell imaging, which was reported previously by us.[32] In this method, the copper-free click reaction would allow conjugation between the azide moiety on the protein substrates and the alkynyl-O-NBD probe, which subsequently triggers the intramolecular nucleophilic substitution by free amines of neighboring lysine residues to turn on the fluorescence of the N-NBD group. Briefly, after incubating HeLa cells with 2.5 mM 3AZ-CoA for 12 h, the cells were washed with PBS and then incubated with 50 μM alkynyl-O-NBD probe (PN-3) for another 2 h. The cells were rinsed to remove any excess reagents and then subjected to fluorescence imaging on a Zeiss LSM 710 Confocal Microscope. As shown in Figure 5, a green fluorescence signal was detected with the treatment of 3AZ-CoA and the fluorescence probe PN-3. In contrast, incubation with the 3AZ-CoA or PN-3 probe alone resulted in no detectable fluorescence. These exciting results were consistent with the in-gel streptavidin-HRP chemiluminescence imaging shown in Figure 4B–D. These observations further corroborate that 3AZ-CoA can be applied as a cell-permeable bio-orthogonal reporter to label intracellular proteins in living cells.

Labeling of HAT1 Substrates in Living Cells. Encouraged by the biochemical and cellular data that showed the bio-orthogonal histone H4 labeling activity of HAT1-Y282A with 3AZ-CoA, and that 3AZ-CoA exhibited excellent cell membrane permeability, we then investigated if HAT1-Y282A matched with 3AZ-CoA could label HAT1 substrates under the native cellular environment. The working scheme is depicted in Figure 6A: first, HEK293T cells were transiently transfected with the full-length HAT1-Y282A plasmid in the expression vector pReceiver-M11 (GeneCopoeia). After 36 h of incubation to allow the cells to express the mutant HAT1, the cells were treated with 2.5 mM 3AZ-CoA and grew for

https://doi.org/10.1021/acschembio.1c00935
ACS Chem. Biol. XXXX, XXX, XXX−XXX

another 12 h. The cells were then lysed and the cell lysate was extracted to conjugate with alkyne-biotin by the CuAAC reaction. Next, the biotinylated proteins were visualized by streptavidin-HRP (Figure 6B). No labeling was seen from the control cells, which had no reporter treatment. Importantly, compared to the 3AZ-CoA treatment alone, multiple darker bands showed up when 3AZ-CoA treatment was combined with HAT1-Y282A overexpression. This indicates that the HAT1-Y282A catalyzed the enzymatic reaction to transfer the 3-azidopropanoyl group from 3AZ-CoA to its corresponding protein substrates under the native cellular environment. This prompted us to enrich the labeled proteins from the cell lysate mixture to identify HAT1 substrates. For this purpose, a cleavable alkyne-diazo-biotin probe was used to conduct the CuAAC reaction, connecting labeled proteins to the biotin handle. After the pull-down experiment on streptavidin-coated beads, the enriched proteins were eluted with sodium dithionite, resolved on SDS-PAGE, and imaged by silver staining (Figure 6C). As expected, much more proteins were enriched from cells with the HAT1-Y282A overexpression and 3AZ-CoA co-treatment, while 3AZ-CoA treatment alone led to less enriched proteins. This demonstrates that our strategy of engineering HAT1 paired with its cell-permeable bio-orthogonal reporter is highly effective for substrate labeling and identification from the native cellular environment.

Proteomic Profiling of HAT1 Substrates by SILAC-MS/MS and Functional Annotation. To discover HAT1 substrates in their native cellular environment, we adopted a quantitative chemoproteomic strategy by using stable isotope labeling of amino acids in cell culture (SILAC) in combination with high-resolution mass spectrometry. The workflow is illustrated in Figure 7A. HEK293T cells were cultured in "light" (medium containing natural arginine and lysine) and "heavy" (medium containing ^{13}C-,^{15}N-substituted arginine and lysine) medium separately. In the "light" medium, the cells were transfected with the full-length HAT1-Y282A plasmid, whereas in the "heavy" medium, the cells were incubated with the empty vector as a negative control. After 36 h of incubation, both cells were treated with 2.5 mM 3AZ-CoA and incubated for another 12 h. Next, the cells were lysed and the cell lysates were pooled together. The proteins were captured by the aforementioned CuAAC reaction and streptavidin pull-down. After trypsin digestion of the enriched proteins, the collected peptides were analyzed by liquid chromatography with tandem mass spectrometry (LC-MS/MS). To ensure the reliability of the results, two biological replicate experiments were performed. Proteins were considered as HAT1 substrates following the ratio light/heavy >2. Among the total identified 1391 protein targets (Supporting Table S2), 123 proteins (Supporting Table S3) were meeting the threshold requirement. Histone H4 was identified among the labeled proteins, which is consistent with our knowledge that HAT1 can acetylate histone H4 at lysine residues 5 and 12.[6,8] Recent study has found that HAT1 is capable to acetylate histone H2A at lysine 5, and in our protein list of HAT1 substrates, the histone H2A was also highly enriched.[9] These identified proteins were also compared with a previously published work that revealed HAT1-dependent protein targets. Garcia et al. identified 65 proteins from embryonic fibroblast cells by HAT1 knockout and used antibody-based enrichment to capture the acetylated proteins that are dependent on HAT1.[13] Of note, 12 of the 65 proteins were found exactly the same or belonging to the same family in our work including H4, H2A, H2B, TPR, PPP2R2A, HSD17B, HMG, HSP, DDX, ATP6V, hnRNP, and NCL (Figure 7B). Importantly, we identified 111 new distinct protein substrates. This could be owing to differences in the cell line type and the higher sensitivity of our method.

To confirm the HAT1 substrates identified in our proteomic results, we chose two undefined HAT1 substrates for further validation through immunoprecipitation and western blotting: human high mobility group box 2 (HMGB2) and human serine/arginine-rich splicing factor 1 (SRSF1). Each plasmid (Myc-DDK-HMGB2, Myc-DDK-SRSF1) was transiently transfected to HEK293T cells and overexpressed with or without HAT1 overexpression. The DDK tagged proteins were immunoprecipitated on Protein G PLUS-agarose resin, and the acetylation levels of the proteins were detected with western blot using pan antiacetyllysine antibody. As shown in Supporting Figure S8, the acetylation signals in both HMGB2 and SRSF1 proteins increased with the presence of HAT1 overexpression, which validates that HAT1 acetylates these two proteins in cells.

The broad-spectrum profiling of HAT1 substrates prompted us to examine its biological involvement and annotate its physiological functions. To this end, the 123 HAT1 substrates were subject to bioinformatics analysis using the DAVID web tool.[33] The gene ontology analysis of the HAT1 substrates shows that HAT1 is involved in a plethora of cellular pathways including transcription, translation, RNA splicing, RNA processing, protein folding, oxidation−reduction process, mitochondrial regulation, etc (Figure 7C). It is not surprising that canonical cellular functions of KATs such as translation initiation, RNA processing, and transcriptional regulation were found in the functional annotation. For example, EIF5B and EIF2S1 play important roles in translation initiation,[34] and acetylation of these proteins may alter their activities. Of note, RNA splicing and RNA processing are among the prominent cellular functions of identified HAT1 substrates.

Through interacting with their binding partners, proteins can carry out their specific functions. We thus analyzed the interaction network of the identified HAT1 substrates (Figure 7D). Consistent with the pathway analysis in Figure 7C, a large majority of the identified HAT1 substrates are binding with proteins, or RNA with 96 and 64 protein substrates. Interestingly, we found that 18 of the HAT1 substrates are binding with ATP such as ATP2A2 and DDX, suggesting that HAT1 might play a role in energy metabolism to drive intracellular biochemical reactions. Ubiquitin is an important small regulatory protein, which can trigger protein degradation, DNA repair, apoptosis, and signal transduction.[35] Alteration of protein ubiquitylation often leads to severe pathological conditions.[36] Importantly, we found that 6 of the HAT1 substrates including CUL1, HSPA5, HSPA9, HSPD1, SCAMP3, and UBE2O are binding with the ubiquitin protein ligase enzyme, suggesting the involvement of HAT1 in protein ubiquitination. We also found 4 HAT1 substrates' binding with protein kinase C, e.g., C1QBP, DSP, GLRX3, and PRKCSH. RPKCSH is a known substrate for protein kinase C, which is associated with polycystic liver disease.[37] The finding of RPKCSH as a HAT1 substrate may provide another possible mechanism for regulatory liver disease.

We also performed a cellular localization analysis of the HAT1 substrates (Figure 7E). We found that 49 of the HAT1 substrates are localized in the nucleus, 39 are in the cytosol, and 27 are distributed in the mitochondrion with some of

https://doi.org/10.1021/acschembio.1c00935
ACS Chem. Biol. XXXX, XXX, XXX−XXX

them overlapping. Therefore, functions of HAT1 clearly go beyond nuclear cellular processing. Overall, these functional annotations suggest that HAT1 substrates have wide distribution for cellular regulation, which further demonstrates that HAT1 is not only involved in histone modification and chromatin regulation but also in many other important cellular biological functions.

Coenzyme A and acyl-CoA are generally considered lacking cell permeability and eukaryotic cells obtain CoA from their extracellular precursors such as vitamin B5.[38] After the uptake of vitamin B5, the molecule will be metabolized and converted into CoA via an evolutionarily conserved five-step enzymatic reaction.[39] Nevertheless, Srinivasan et al. demonstrated that exogenous CoA could also serve as a source for mammalian cells or organisms to adjust intracellular CoA levels: one possible mechanism is that CoA could be hydrolyzed into a more stable molecule, 4′-phosphopantetheine, extracellularly near the cell membrane, which then penetrates the cell membrane by passive diffusion. Once entering the cell, 4′-phosphopantetheine is enzymatically converted to CoA by CoA synthases.[31] Later, the same group further demonstrated that acetylated 4′-phosphopantetheine is also stable and possesses cell permeability to serve as a source for the intracellular Ac-CoA level.[40] These findings provide an important understanding of CoA compounds entering the cell and may suggest a possible pathway for 3AZ-CoA and 4AZ-CoA entering the cell, which subsequently labels cellular protein substrates of HATs (Supporting Figure S9). However, mechanism studies will be needed to investigate the details of how the two acyl-CoA reporters get into cells. In principle, experiments would be required to determine whether these reporters can be hydrolyzed in the cell culture medium and enter the cells by passive diffusion or whether there is any specific transporter to facilitate their entry across the cell membrane. Compared to the alkyne acyl-CoA, 3AZ-CoA and 4AZ-CoA showed a better labeling efficiency (Figure 4B). The reason for this distinction in cellular protein labeling is still elusive at this stage and warrants mechanistic investigation.

We have identified more than 100 protein substrates of HAT1 by combining bio-orthogonal labeling and SILAC proteomics, with 12 being previously known and 111 first-time disclosed. We also validated two novel substrates of HAT1: HMGB2 and SRSF1 with transfection experiments. These findings greatly broaden the scope of the biological function of HAT1, which is far beyond histone modification and chromatin regulation. The separated binding sites in HAT1 for Ac-CoA and peptide substrates[28] ensure that a mutation in the Ac-CoA binding pocket of HAT1 has a low possibility to change the binding specificity of protein substrates. From our previous work, some wild-type HATs such as p300 can also utilize 3AZ-CoA to transfer the azido group to its protein substrates.[24,25] Therefore, some of the labeled proteins appearing in the absence of HAT1-Y282A overexpression may be substrates of other HATs. Future research is needed to characterize detailed acetylation sites in the found HAT1 substrates and study their biochemical outcome in protein function regulation.

CONCLUSIONS

In summary, we have established a bio-orthogonal proteomic methodology to quickly and reliably detect protein substrates of an individual KAT in living cells. We generated HAT1 mutants (e.g., HAT1-Y282A) through rational engineering that can accommodate clickable acyl-CoA reporters for substrate labeling. Meanwhile, we identified 3AZ-CoA to be a cell-permeable bio-orthogonal reporter for protein acylation. Piecing the KAT−acyl-CoA bio-orthogonal labeling pair together with SILAC proteomics, we successfully profiled more than 100 substrates of HAT1 in the native cellular environment. This finding that HAT1 targets numerous nonhistone cellular protein substrates greatly broadens the scope of biological modalities regulated by HAT1, which is far beyond the chromatin realm. The bio-orthogonal chemo-proteomic strategy demonstrated here would be complementary and advantageous for the detection and profiling of cellular protein substrates of other KAT members in the native biological contexts.

METHODS

Mutation of HAT1 DNA and Protein Expression and Purification. The wild-type pET28a-HAT1(20−341) plasmid was obtained from Addgene (plasmid# 25239). The wild-type DNA plasmid was used as a template to mutate all of the selected sites. HAT1 mutants were produced by first designing forward and reverse primers containing the desired single-point mutation. The forward and reverse primers used to generate the single-point mutants are listed in Supporting Table S1. Next, by using the QuikChange procedure (Stratagene), the target site-directed mutation was introduced into the HAT1 plasmid. Once all of the ingredients were added, the sample was preheated at 95 °C for 5 min, and then, the polymerase chain reaction (PCR) method was followed: First, the temperature increased to 95 °C for 1 min for the denaturation of the double-stranded plasmid. Next, the annealing of the primers occurred when the temperature decreased to 55 °C for 1 min. Finally, the extension occurred when the temperature was at 68 °C for 16.5 min. The cycle was repeated 17 times, and then, the template DNA was digested with the Dpn I restriction enzyme. Transformation was then carried out using the PCR product and *E. coli* XL1-Blue competent cells. The next day, colonies were selected and grown at 37 °C overnight in LB media supplemented with kanamycin (0.125 mg mL^{-1}). Plasmids were purified using the Promega Wizard plus Miniprep system. DNA sequencing confirmed that all intended mutations occurred as desired.

The expression and purification of HAT1 (20−341) and HAT1 mutants were done following the method described by Wu et al.[28] Briefly, the proteins were expressed in *E. coli* and purified using the Ni-NTA resin. Transformation was done in *E. coli* BL21-CodonPlus (DE3)-RIL competent cells using the heat-shock method, and then, the cells were spread on agar plates containing antibiotics kanamycin and chloramphenicol. Protein expression was induced by the addition of 1 mM isopropyl β-D-1-thiogalactopyranoside (IPTG) and shaken for 16 h at 16 °C. The cells were collected and suspended in the lysis buffer (50 mM Na-phosphate (pH 7.4), 250 mM NaCl, 5 mM imidazole, 5% glycerol, 2 mM β-mercaptoethanol, and 1 mM phenylmethanesulfonyl fluoride (PMSF)) and then disrupted using the Microfluidics cell disruptor. The supernatant was passed through a column containing Ni-NTA resin equilibrated with column washing buffer (20 mM HEPES pH 8, 250 mM NaCl, 5% glycerol, 30 mM imidazole, and 1 mM PMSF) and the resin was washed with column washing buffer. Next, the resin was washed with the buffer containing a higher concentration of imidazole (20 mM HEPES, pH 8, 250 mM NaCl, 5% glycerol, 50 mM imidazole, and 1 mM PMSF). Finally, HAT1 was eluted with elution buffer (20 mM HEPES, pH 8, 250 mM NaCl, 5% glycerol, 500 mM imidazole, and 1 mM PMSF). The eluent fractions were further checked by SDS-PAGE, and the enzyme concentrations were determined by the Bradford assay. Enzymes were aliquoted and stored at −80 °C for future use.

Fluorogenic CPM Assay to Screen HAT1 Mutant Activity. The acylation activity of HAT1 and HAT1 mutants was analyzed using the CPM assay. To screen the various HAT1 mutants against the acyl-CoA analogues, reactions contained 0.04 μM enzyme, H4 (1-

https://doi.org/10.1021/acschembio.1c00935
ACS Chem. Biol. XXXX, XXX, XXX−XXX

20) peptide (40 μM), and acyl-CoA analogues (20 μM). Samples were incubated for 1 h at 30 °C. Evaluation of HAT1-Y282A kinetics was also done using the CPM assay with reactions carried out at 30 °C for 15 min and sample conditions were as follows: 0.04 μM enzyme, H4 (1-20) peptide (200 μM), and acyl-CoA analogues (0−200 μM). All reactions were quenched by the addition of an excessive amount of 7-diethylamino-3-(4′-maleimidylphenyl)-4-methylcoumarin (CPM) dissolved in DMSO and then incubated in total darkness for 20 min in room temperature. For the kinetics assay, 203 μM (final) CPM was used when acyl-CoA analogue concentrations varied from 0 to 200 μM. When the acyl-CoA analogue concentration was fixed at 20 μM, 30 μM (final) CPM was used. Fluorescence was measured at an excitation and emission wavelength of 392 and 482 nm, respectively.

Normal and SILAC HEK293T Cell Culture. For normal HEK293T cell culture, cells were cultured in Dulbecco's modified Eagle medium (DMEM) supplemented with 10% fetal bovine serum (FBS, Life Technologies) and 1% penicillin−streptomycin (15140122, ThermoFisher Scientific). For SILAC HEK293T cell culture, cells were cultured in DMEM (arginine and lysine free, Life Technologies) supplemented with 10% dialyzed FBS (Life Technologies), 1% penicillin−streptomycin containing either 22 or 55 mg L^{-1} nonlabeled arginine and lysine, or 22 mg L^{-1} $^{13}C_6{}^{15}N_4$-arginine and 68 mg L^{-1} $^{13}C_6{}^{15}N_2$-lysine (Cambridge Isotope Laboratories). The SILAC cells were cultured for at least 8 passages before any experiments. All of the cells were maintained at 37 °C with 5% CO_2.

Transient Transfection of HAT1-Y282A and Bio-orthogonal Reporter Treatment for HAT1 Substrate Labeling. A full-length HAT1-Y282A-encoding sequence was inserted into the M11 vector to generate a HAT1-Y282A overexpression plasmid for the mammalian cell. HEK293T cells were cultured to reach around 60% confluence stage, and transient transfection of the plasmid HAT1-Y282A was conducted by Lipofectamine 3000 (ThermoFisher SCIENTIFIC, Product #L3000008) according to the manufacture's protocol followed by 36 h of incubation. Next, cells were treated with 2.5 mM 3AZ-CoA to induce the protein labeling. After another 12 h of incubation, the cells were washed with ice-cold PBS and harvested and lysed by ice-cold M-PER buffer containing a 1% protease inhibitor cocktail. The protein was then collected and the protein concentration was determined as described above. The protein solution was used for further click reaction and streptavidin detection.

Protein Labeling by CuAAC Reaction and Streptavidin Detection. Thirty micrograms of the cell lysate protein mixture was mixed with a click cocktail containing 50 μM alkyne-biotin or diazo biotin alkyne, 2.5 mM sodium ascorbate, 0.5 mM copper sulfate, and 0.25 mM ligand BTTAA. After incubation in room temperature for 1 h, 1× loading dye was added and boiled for 5 min. The samples were then resolved on 4−20% SDS-PAGE gradient gel. The separated proteins were transferred to a nitrocellulose membrane and blocked with 5% nonfat milk for 1 h. The membrane was incubated with streptavidin-HRP for another 1 h and scanned by a chemiluminescence scanner.

Streptavidin affinity enrichment and sample preparation for mass spectrometry. Six hundred micrograms of the cell lysate was incubated with the click cocktail as described above to conduct biotinylation of the target protein. Excess diazo biotin alkyne was removed by spin dialysis. High-capacity streptavidin agarose was first equilibrated by PBS and then incubated with the sample for 1 h with gentle agitation. Next, the resins were collected by centrifugation at 5000*g* for 5 min and washed with PBS supplemented with 0.2% (w/v) SDS, PBS supplemented with 0.1% (w/v) SDS and 6 M urea, and 50 mM NH_4HCO_3 supplemented with 0.1% SDS. Then, the resins were incubated with 30 mM $Na_2S_2O_4$ in 50 mM NH_4HCO_3 for 1 h to elute the protein off the beads. The mixture was then centrifuged at 5000*g* for 5 min and the supernatant was collected and dried by SpeedVac for further analysis. The dried protein sample was dissolved in 30 μL of water followed by incubation with 20 mM DTT at 75 °C for 15 min and 200 mM iodoacetamide in room temperature for 20 min.

■ ASSOCIATED CONTENT

Supporting Information

The Supporting Information is available free of charge at https://pubs.acs.org/doi/10.1021/acschembio.1c00935.

Additional experimental methods on organic synthesis, bio-orthogonal labeling characterizations, cellular assays, and proteomics. Supporting Figures S1−S9 contain information on SDS-PAGE of recombinant HAT1 proteins, activities of HAT1 mutants, mass spectrometry and in-gel imaging characterization of peptide acylations, kinetic measurement of HAT1-Y282A activity, metabolite and toxicity analysis of 3AZ-CoA in cells, and HAT1 substrate validation. Supporting Table S1 contains the primer information in HAT1 mutagenesis, and Tables S2 and S3 show the list of proteins identified from chemoproteomic measurements (PDF)

(xlsx)

■ AUTHOR INFORMATION

Corresponding Author

Y. George Zheng − *Department of Pharmaceutical and Biomedical Sciences, College of Pharmacy, University of Georgia, Athens, Georgia 30602, United States;* orcid.org/0000-0001-7116-3067; Phone: (706) 542-0277; Email: yzheng@uga.edu; Fax: (706) 542-5358

Authors

Jiabao Song − *Department of Pharmaceutical and Biomedical Sciences, College of Pharmacy, University of Georgia, Athens, Georgia 30602, United States*

Liza Ngo − *Department of Pharmaceutical and Biomedical Sciences, College of Pharmacy, University of Georgia, Athens, Georgia 30602, United States*

Kaylyn Bell − *Department of Pharmaceutical and Biomedical Sciences, College of Pharmacy, University of Georgia, Athens, Georgia 30602, United States*

Complete contact information is available at: https://pubs.acs.org/10.1021/acschembio.1c00935

Notes

The authors declare no competing financial interest.

■ ACKNOWLEDGMENTS

The authors acknowledge Dr. J. Qiao for the help with confocal imaging. They thank the Proteomics and Mass Spectrometry facility (PAMS) at UGA for the peptide MS support. They also acknowledge the Mass Spectrometry and Proteomics Core on the Scripps Research Florida campus for the SILAC-MS/MS analysis. This work was supported by the National Science Foundation (grants 1507741 and 1808087 to Y.G.Z.).

■ REFERENCES

(1) Ali, I.; Conrad, R. J.; Verdin, E.; Ott, M. Lysine Acetylation Goes Global: From Epigenetics to Metabolism and Therapeutics. *Chem. Rev.* **2018**, *118*, 1216−1252.

(2) Sinclair, W. R.; Shrimp, J. H.; Zengeya, T. T.; Kulkarni, R. A.; Garlick, J. M.; Luecke, H.; Worth, A. J.; Blair, I. A.; Snyder, N. W.; Meier, J. L. Bioorthogonal pro-metabolites for profiling short chain fatty acylation. *Chem. Sci.* **2018**, *9*, 1236−1241.

(3) Kim, S. C.; Sprung, R.; Chen, Y.; Xu, Y.; Ball, H.; Pei, J.; Cheng, T.; Kho, Y.; Xiao, H.; Xiao, L.; et al. Substrate and functional diversity

of lysine acetylation revealed by a proteomics survey. *Mol. Cell* **2006**, *23*, 607−618.
(4) Song, J.; Zheng, Y. G. Bioorthogonal Reporters for Detecting and Profiling Protein Acetylation and Acylation. *SLAS Discovery* **2020**, *25*, 148−162.
(5) Marmorstein, R.; Zhou, M. M. Writers and readers of histone acetylation: structure, mechanism, and inhibition. *Cold Spring Harbor Perspect. Biol.* **2014**, *6*, No. a018762.
(6) Kleff, S.; Andrulis, E. D.; Anderson, C. W.; Sternglanz, R. Identification of a gene encoding a yeast histone H4 acetyltransferase. *J. Biol. Chem.* **1995**, *270*, 24674−24677.
(7) Poziello, A.; Nebbioso, A.; Stunnenberg, H. G.; Martens, J. H. A.; Carafa, V.; Altucci, L. Recent insights into Histone Acetyltransferase-1: biological function and involvement in pathogenesis. *Epigenetics* **2021**, *16*, 838−850.
(8) Verreault, A.; Kaufman, P. D.; Kobayashi, R.; Stillman, B. Nucleosomal DNA regulates the core-histone-binding subunit of the human Hat1 acetyltransferase. *Curr. Biol.* **1998**, *8*, 96−108.
(9) Tafrova, J. I.; Tafrov, S. T. Human histone acetyltransferase 1 (Hat1) acetylates lysine 5 of histone H2A in vivo. *Mol. Cell. Biochem.* **2014**, *392*, 259−272.
(10) Parthun, M. R. Hat1: the emerging cellular roles of a type B histone acetyltransferase. *Oncogene* **2007**, *26*, 5319−5328.
(11) Weinert, B. T.; Narita, T.; Satpathy, S.; Srinivasan, B.; Hansen, B. K.; Scholz, C.; Hamilton, W. B.; Zucconi, B. E.; Wang, W. W.; Liu, W. R.; et al. Time-Resolved Analysis Reveals Rapid Dynamics and Broad Scope of the CBP/p300 Acetylome. *Cell* **2018**, *174*, 231−244.
(12) Huang, H.; Tang, S.; Ji, M.; Tang, Z.; Shimada, M.; Liu, X.; Qi, S.; Locasale, J. W.; Roeder, R. G.; Zhao, Y.; et al. p300-Mediated Lysine 2-Hydroxyisobutyrylation Regulates Glycolysis. *Mol. Cell* **2018**, *70*, 663−678.
(13) Garcia, P. A. A.; Nagarajan, P.; Parthun, M. R. Hat1-Dependent Lysine Acetylation Targets Diverse Cellular Functions. *J. Proteome Res.* **2020**, *19*, 1663−1673.
(14) Shaw, P. G.; Chaerkady, R.; Zhang, Z.; Davidson, N. E.; Pandey, A. Monoclonal antibody cocktail as an enrichment tool for acetylome analysis. *Anal. Chem.* **2011**, *83*, 3623−3626.
(15) Huang, H.; Wang, D. L.; Zhao, Y. Quantitative Crotonylome Analysis Expands the Roles of p300 in the Regulation of Lysine Crotonylation Pathway. *Proteomics* **2018**, *18*, No. 1700230.
(16) Han, Z.; Wu, H.; Kim, S.; Yang, X.; Li, Q.; Huang, H.; Cai, H.; Bartlett, M. G.; Dong, A.; Zeng, H.; et al. Revealing the protein propionylation activity of the histone acetyltransferase MOF (males absent on the first). *J. Biol. Chem.* **2018**, *293*, 3410−3420.
(17) Zhu, Z.; Han, Z.; Halabelian, L.; Yang, X.; Ding, J.; Zhang, N.; Ngo, L.; Song, J.; Zeng, H.; He, M.; et al. Identification of lysine isobutyrylation as a new histone modification mark. *Nucleic Acids Res.* **2021**, *49*, 177−189.
(18) Yang, G.; Yuan, Y.; Yuan, H.; Wang, J.; Yun, H.; Geng, Y.; Zhao, M.; Li, L.; Weng, Y.; Liu, Z.; et al. Histone acetyltransferase 1 is a succinyltransferase for histones and non-histones and promotes tumorigenesis. *EMBO Rep.* **2021**, *22*, No. e50967.
(19) Delaney, K.; Tan, M.; Zhu, Z.; Gao, J.; Dai, L.; Kim, S.; Ding, J.; He, M.; Halabelian, L.; Yang, L.; et al. Histone lysine methacrylation is a dynamic post-translational modification regulated by HAT1 and SIRT2. *Cell Discovery* **2021**, *7*, No. 122.
(20) He, M.; Han, Z.; Liu, L.; Zheng, Y. G. Chemical Biology Approaches for Investigating the Functions of Lysine Acetyltransferases. *Angew. Chem., Int. Ed.* **2018**, *57*, 1162−1184.
(21) Yu, M.; de Carvalho, L. P.; Sun, G.; Blanchard, J. S. Activity-based substrate profiling for Gcn5-related N-acetyltransferases: the use of chloroacetyl-coenzyme A to identify protein substrates. *J. Am. Chem. Soc.* **2006**, *128*, 15356−15357.
(22) Lyu, Z.; Zhao, Y.; Buuh, Z. Y.; Gorman, N.; Goldman, A. R.; Islam, M. S.; Tang, H. Y.; Wang, R. E. Steric-Free Bioorthogonal Labeling of Acetylation Substrates Based on a Fluorine-Thiol Displacement Reaction. *J. Am. Chem. Soc.* **2021**, *143*, 1341−1347.
(23) Yang, Y. Y.; Ascano, J. M.; Hang, H. C. Bioorthogonal chemical reporters for monitoring protein acetylation. *J. Am. Chem. Soc.* **2010**, *132*, 3640−3641.
(24) Han, Z.; Chou, C. W.; Yang, X.; Bartlett, M. G.; Zheng, Y. G. Profiling Cellular Substrates of Lysine Acetyltransferases GCN5 and p300 with Orthogonal Labeling and Click Chemistry. *ACS Chem. Biol.* **2017**, *12*, 1547−1555.
(25) Yang, C.; Mi, J.; Feng, Y.; Ngo, L.; Gao, T.; Yan, L.; Zheng, Y. G. Labeling lysine acetyltransferase substrates with engineered enzymes and functionalized cofactor surrogates. *J. Am. Chem. Soc.* **2013**, *135*, 7791−7794.
(26) Islam, K. The Bump-and-Hole Tactic: Expanding the Scope of Chemical Genetics. *Cell Chem. Biol.* **2018**, *25*, 1171−1184.
(27) Radziwon, K.; Weeks, A. M. Protein engineering for selective proteomics. *Curr. Opin. Chem. Biol.* **2021**, *60*, 10−19.
(28) Wu, H.; Moshkina, N.; Min, J.; Zeng, H.; Joshua, J.; Zhou, M. M.; Plotnikov, A. N. Structural basis for substrate specificity and catalysis of human histone acetyltransferase 1. *Proc. Natl. Acad. Sci.* **2012**, *109*, 8925−8930.
(29) Gao, T.; Yang, C.; Zheng, Y. G. Comparative studies of thiol-sensitive fluorogenic probes for HAT assays. *Anal. Bioanal. Chem.* **2013**, *405*, 1361−1371.
(30) Trievel, R. C.; Li, F. Y.; Marmorstein, R. Application of a fluorescent histone acetyltransferase assay to probe the substrate specificity of the human p300/CBP-associated factor. *Anal. Biochem.* **2000**, *287*, 319−328.
(31) Srinivasan, B.; Baratashvili, M.; van der Zwaag, M.; Kanon, B.; Colombelli, C.; Lambrechts, R. A.; Schaap, O.; Nollen, E. A.; Podgorsek, A.; Kosec, G.; et al. Extracellular 4′-phosphopantetheine is a source for intracellular coenzyme A synthesis. *Nat Chem Biol* **2015**, *11*, 784−792.
(32) He, M.; Han, Z.; Qiao, J.; Ngo, L.; Xiong, M. P.; Zheng, Y. G. A bioorthogonal turn-on fluorescent strategy for the detection of lysine acetyltransferase activity. *Chem Commun (Camb)* **2018**, *54*, 5594−5597.
(33) Huang, D. W.; Sherman, B. T.; Lempicki, R. A. Systematic and integrative analysis of large gene lists using DAVID bioinformatics resources. *Nat. Protoc.* **2009**, *4*, 44−57.
(34) Smith, R. C. L.; Kanellos, G.; Vlahov, N.; Alexandrou, C.; Willis, A. E.; Knight, J. R. P.; Sansom, O. J. Translation initiation in cancer at a glance. *J. Cell Sci.* **2021**, *134*, No. jcs248476.
(35) Pickart, C. M.; Eddins, M. J. Ubiquitin: structures, functions, mechanisms. *Biochim. Biophys. Acta* **2004**, *1695*, 55−72.
(36) Deng, L.; Meng, T.; Chen, L.; Wei, W.; Wang, P. The role of ubiquitination in tumorigenesis and targeted drug discovery. *Signal Transduction Targeted Ther.* **2020**, *5*, No. 11.
(37) Li, A.; Davila, S.; Furu, L.; Qian, Q.; Tian, X.; Kamath, P. S.; King, B. F.; Torres, V. E.; Somlo, S. Mutations in PRKCSH cause isolated autosomal dominant polycystic liver disease. *Am. J. Hum. Genet.* **2003**, *72*, 691−703.
(38) Sibon, O. C.; Strauss, E. Coenzyme A: to make it or uptake it? *Nat. Rev. Mol. Cell Biol.* **2016**, *17*, 605−606.
(39) Leonardi, R.; Zhang, Y. M.; Rock, C. O.; Jackowski, S. Coenzyme A: back in action. *Prog. Lipid Res.* **2005**, *44*, 125−153.
(40) Di Meo, I.; Colombelli, C.; Srinivasan, B.; de Villiers, M.; Hamada, J.; Jeong, S. Y.; Fox, R.; Woltjer, R. L.; Tepper, P. G.; Lahaye, L. L.; et al. Acetyl-4′-phosphopantetheine is stable in serum and prevents phenotypes induced by pantothenate kinase deficiency. *Sci. Rep.* **2017**, *7*, No. 11260.

https://doi.org/10.1021/acschembio.1c00935
ACS Chem. Biol. XXXX, XXX, XXX−XXX